DOI: http://dx.doi.org/10.15407/tpwj2019.01.06

ROBOTIC WELDING ON TUBE NODES

S. KEITEL[1]**, U. MÜCKENHEIM**[1]**, U. WOLSKI**[1]**, S. LOTZ**[1]**, J. MÜGLITZ**[2] and **T. SIGMUND**[3]
[1]SLV Halle GmbH, Halle, Germany
[2]ZIS Industrietechnik GmbH, Meerane , Germany
[3]Ibs Automation GmbH, Chemnitz. E-mail: mail@slv-hall.de

Hollow-profile structures are significantly more stable than structures made using open profiles, which is the main reason for their use in truss and truss-like structures. The node intersections of such structures requires three-dimensional curved welded joints. Small and medium-sized enterprises usually weld tubular frame and truss structures manually, which is highly time-consuming and cost-intensive. In addition, this method requires personnel with corresponding qualifications to carry out the work as the welders need to adapt to constantly changing conditions in weld preparation and welding position, which obviously requires intensive training. Replacing this manual activity by mechanised welding processes would provide great relief to welders. 1 Ref., 2 Tables, 8 Figures.

Keywords: *hollow-profiles, robotsystem, sensor, MAG, productivity; 3D-welding; 3D-cutting*

One-off production still dominates in steel construction as there is hardly any standardisation in joints as applies in other applications, such as pipeline construction. This has kept series production on hollow profile nodes out of the focus in research and development. However, the situation has changed in recent years especially due to developments in offshore wind farms. These structures have frequently repeating joints at the nodes, so a process would be conceivable involving prefabricated nodes with beams welded in between the nodes on site using orbital welding processes. Node prefabrication using the corresponding equipment and manipulation automation would be realistic in view of the small size that nodes occupy compared to the overall structure. Even so, tube node joint welding has so far only been fully mechanised to a limited extent in practice. The equipment is almost only programmed using teach-in methods. Technological limits exist in applications such as those involving multilayer welds and excessive tolerances in semi-finished structures, especially in fully mechanised root welds. Hollow profile prefabrication, on the other hand, involves CNC-controlled thermal cutting using offline programming.

This was the point of focus in the research project, which used theoretical studies, systematisation, welding process development, software customisation, and experimental production on a test rig for industrial implementation towards developing a decision-making basis with presentable reference solutions.

Defining the general conditions. *Tube node geometries and dimensions*. The studies included lattice boom structures in crane construction, tube nodes in vehicle construction and nodes in offshore constructions. These industries all share similar node structures, albeit in varying dimensions. Diameters range from 40 mm to 300 mm in typical structures, with wall thicknesses varying from around 2 to 16 mm.

All the nodes shared a full joint to the socket on the entire wall thickness with added fillet welds. The following materials and tube dimensions were selected for the nodes as examples based on offshore construction applications:

- main tube: diameter 406.4×10 mm; socket: diameter 273×16 mm;
- material: S355;
- oblique joint: 45°, T-joint: 90°;
- bevel angle: 50°.

Weld preparation. Flame or plasma cutting may be used on tube sections in the offshore industry due to the materials and wall thicknesses used. Autogenous flame cutting is usually used in this thickness range, and was also used in the studies. The main reason for that is that flame cutting is suitable for very large cutting angles of up to 65°. Machining processes were also considered in weld preparation, beginning with considering a possible saving in costs especially with thin walls by eliminating the reworking required on thermally cut surfaces and higher accuracy of fit between the components to be joined, even with the increased costs of thin walls. Machining would reduce tolerances to about ± 0.5 mm as compared to about ±2 mm for flame cutting sockets at diameters of 273 mm. Sockets cut at angles of 90° and 60° to the main tube were first flame-cut at a dimensional tolerance of 5 mm, and then machined down. This involved setting the main tube contour at 3 mm away from the nominal inner diameter of the socket to achieve a high degree of accuracy, rather than at the inner diameter itself.

The selected K-node was shaped as a full joint throughout the largest part. The intersection contour in the remaining portion was joined using a multilayer fillet weld, but did not cover the whole material thickness of the socket. In contrast, the double T-node required a full joint around the whole circumference.

Welding processes, additives and auxiliaries. MAG welding (135) was used for deposition rates and suitability for difficult welding positions in agreement with representatives from industry. The intersection contour and frequent variations in roundness in the tubes cause different gap dimensions in positioning the connecting tubes to the main tube. One of the project's areas of focus was therefore to study automated root-run welding on varying gap widths. A number of process variants available on the market may be suitable for this problem, which required research. Several process control options were available using a suitable MIG/MAG power source from EWM. The studies were limited to one power source manufacturer so as to ensure the same equipment in the studies at Halle and on the larger tube nodes at the project partner ibs Automation GmbH in Chemnitz. Welding additive: DIN EN ISO 14341 – A – G4Si1; diameter 1.2 mm Inert gas: DIN EN ISO 14175 – M21 – ArC – 18; 15 l/min.

Design and construction of a test rig. Considerations on applicable component geometries included accessibility during welding, working space and load capacities of potentially suitable robots. Another important point was component positioning depending on weld characteristics with the various component geometries.

These general conditions led to the test rig design as shown in Figure 1.

- KR 15/2 robot with 15 kg load capacity;
- one manipulator with 5 m lift to move the robot;
- manually movable and fixable DKP-400 rotary tilting table on a linear axis positioned before the manipulator;
- one manually movable and fixable roller block on the linear axis;
- CNC control for the nine synchronised movable axes connected to a laser triangulation sensor for weld tracking.

The robot was equipped with Sinumerik 840D SolutionLine CNC control as options for integrating sensor systems, and therefore data connections to the tube blanks. CNC control has a more open structure for the integration required compared to robot controllers. The arrangement of the tilt-and-turn table's rotation axis in the lower part of the work space of the robot and the resulting steep angle of the robot's forearm minimised the risk of collision with the component. Apart from that, the main tube was rotated around its central axis on tracking the weld contour, so the contour on the intersection was effectively welded in a single plane allowing the horizontal rotated welding position.

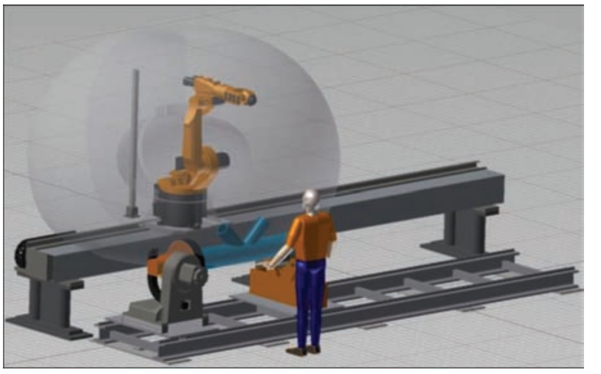

Figure 1. Test rig design with tube nodes

A fixed station with monitor, keyboard, mouse and a machine control panel and a hand-held controller as alternative options are available for CNC operation. An interface controller includes, among other things, safety components for an external emergency-stop circuit and access protection for the work space using a light curtain in automatic mode. Figure 2 shows a partial view of the system with the control components.

Developing welding technologies. Initial welding tests on 20 mm linear oblique weld samples using bevel-groove weld preparation alongside the development phase of the robot system were carried out with a 60° flame angle and 50° bevel angle for parameter determination on varying gap widths on a three-axis portal in horizontal rotated welding position. Gap widths of around 1 to 2.5 mm were bridged using a stringer bead root weld, but existing technology (standard process, no pulsing) was unreliable at welding root gaps of 3 mm. The root was unevenly welded through in parts; we were unable to weld a secure

Figure 2. Partial view of the robot system

Table 1. Process parameters determined for oblique joint samples (pulsed root)

Gap, mm	I_s, A	U_s, V	v_D, m/min	v_s, cm/min	Comment
0	270–280	30,0	9,3	45	Stringer bead
2	140–150	23,0	4,5	40	Stringer bead
3	140–150	23,0	4,5	16	0,8 s pulse, 1.5 mm amplitude
4	140–150	23,0	4,5	11	0,8 s pulse, 3.0 mm amplitude

Table 2. Macrosections for the root weld using the pulsed MAG process

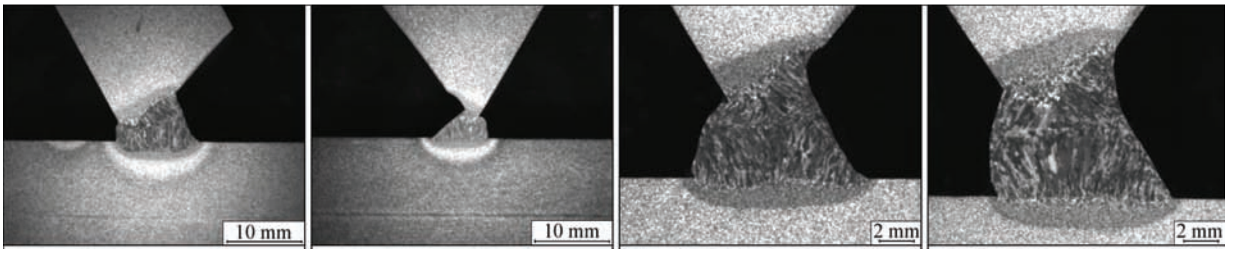

0 mm gap	2 mm gap	3 mm gap	4 mm gap

joint onto the chamfered side of the metal sheet. This bevel-groove weld preparation posed increased risk of incomplete fusion at the root. After starting up the robot work station and connecting a suitable power source using a suitable interface, we made more attempts on a 4 mm gap using methods including the pulse-controlled process and ColdArc light arc. The study focused on determining the parameters for the root weld up to a gap of 4 mm. Samples with gaps of up to 2 mm were still welded wire oscillation, while the torch required oscillation on gaps of 3 mm. We were able to determine suitable parameters for intermediate and outer layers in the preliminary tests on the three-axis portal. In summary, the pulse process proved to be the most suitable root-welding method as shown by detectable level of reliability in edge fusion. The process parameters ultimately defined for the root welds are listed in Table 1. The following Table 2 shows the macrosections for the root welds using the MAG pulse process. Wire oscillation is advisable for reliable fusion on the base plate or tube with root gaps of more than 2 mm. In summary, we opted for the pulse process for the root, intermediate and cover layers in the experiments on the tube nodes.

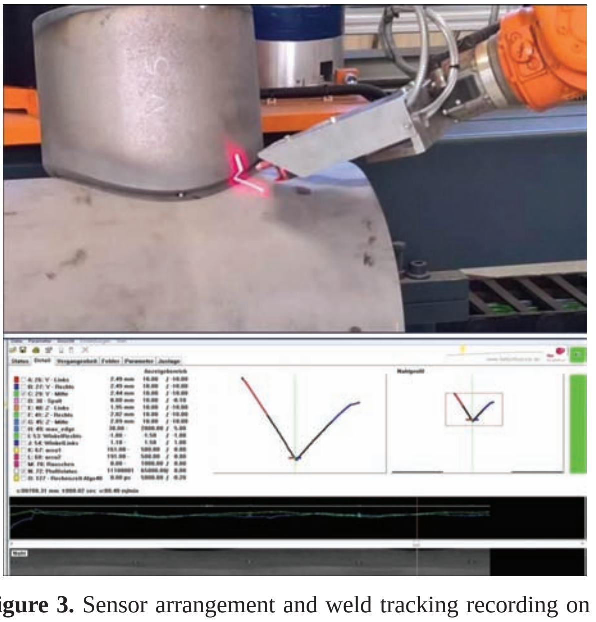

Figure 3. Sensor arrangement and weld tracking recording on a T-joint before welding the root

Control and sensor designs. The robot system's control concept was based on Sinumerik 840D SolutionLine CNC control with Sinumerik Operate 4.7 and Sinamics S120 drive technology from Siemens. These components were designed for operation with a KR15/2 robot and DKP-400 tilt-and-turn table.

The whole approach includes a sensor system consisting of an S7 laser triangulation sensor and a sensor computer from Falldorf. Together with Inspector software, this proved suitable for weld tracking and inspection. Weld tracking used the functions on the gap sensor to determine characteristics of the joint or parts of the joint not yet welded. The joint characteristics were transferred to the CNC controller and processed in real time while the sensor computer received information such as applicable parameters for weld tracking and current path speed from the controller. A Profinet interface was used for communication between the CNC control and sensor computer.

Weld preparation and layer structure required analysis in developing the sensor design. The important point here was to ensure reliable readings for geometric characteristics on the weld joint together with the appropriate evaluation algorithms in the sensor software. Existing geometric characteristics comprised the surfaces on the sheets or tubes, intersections between weld bead and sheet or tube, and intersections between weld layers. Preliminary tests showed evaluation algorithm No.40, T-joint Multimax, to be suitable, as it allowed two lines to be defined around the profile to be imaged. The intersection between the two lines was interpreted as the weld tracking position, and its coordinates were transferred to the CNC control. Additional adjustable offsets in two directions enabled torch position movement against the weld tracking point in addition to the positions of following weld layer on intermediate and cover layers during weld tracking. Smooth metal surfaces are unsuitable for the laser triangulation sensor as surface condition plays a critical role. Sandblasting or brushing the weld preparation or surface in the laser sensor's detection area provides a remedy. The option to decouple welding from measurement proved correct. Figure 3 shows the example of weld tracking on a tube node T-joint

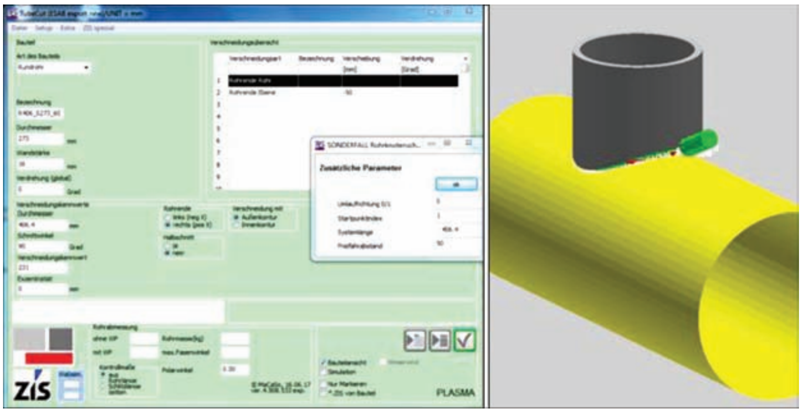

Figure 4. TubeCut input dialogue with rotating direction and starting point as well as a graphical rendering for the T-joint

recorded before a root weld. As the weld filled, usable areas were reduced with decreasing numbers of imaging points available; this made weld tracking more difficult for mathematically modelling the two intersecting lines, at least on the socket side. This evaluation method was unreliable for use on intermediate layers featuring several adjacent welds with a convex profile, which already arose after the third weld layer. Further progress in the multilayer weld saw increasingly varied geometry characteristics due to the uneven filling between the saddle and crown points during inspection tracking. Therefore, the path resulting from weld tracking on the non-welded joint was used for all the weld layers on the welds to the tube nodes and tracked using offset values derived from the layer structure of the oblique joint samples.

Test procedure. First, the weld path was generated using TubeCut CAM software (ZIS Industrietechnik GmbH) [1]. The direction of travel around the socket and the beginning of the path were selectable. A DXF file was suitable for setting the welding torch position and angle to the layer structure. The horizontal rotated welding position was used in welding the socket, which involved using the robot system to turn the tube nodes around the main axis of the tube in sync with the tool. The equipment configuration caused access problems for the welding torch while encircling the oblique joint at the acute angle of the joint. The parameter input dialogue in the customised TubeCut showed more favourable conditions for welding studies on the T-joint as shown in Figure 4.

TubeCut was used again to create the NC program for the T-joint, which only generated the path for the root weld. The path was then used to start weld tracking, the calculated path adjusted to match the actual process, and the coordinates of the path points stored in an NC file for further use. There was no algorithm for parameter adjustment on the widely fluctuating root gap at this point, so the weld preparation was additionally manually adjusted for a root gap from 0 to 0.5 mm. This made the root weld possible at fixed process parameters for a gap of 0 mm at a welding speed adjusted to 40 cm/min. T-joint nodes were also partly mechanically welded to compare cost-effectiveness; Figure 5 shows selected steps in the robot welding process flow.

The small amount of welding material missing at one point on the top layer in the first attempt was solved by minor adjustments in wire positioning; no external irregularities were recognisable in subsequent tests. Figure 6 shows an example image of a cover layer part of a T-joint with a flame-cut and manually altered weld preparation and a total of nine weld layers required.

Welders constantly need to change posture in partly mechanised welding, and each bead required welding in four individual sections (approximately horizontal rotated position). Achieving a favourable weld shape while minimising grinding effort on the intermediate layers required lowering the wire feed and welding current. However, this also required eighteen weld layers.

Results. Three macrosections each were obtained at different positions on the weld for metallographic tests

Figure 5. Steps in the process flow

Figure 6. Tube node weld, T-joint (cover layer)

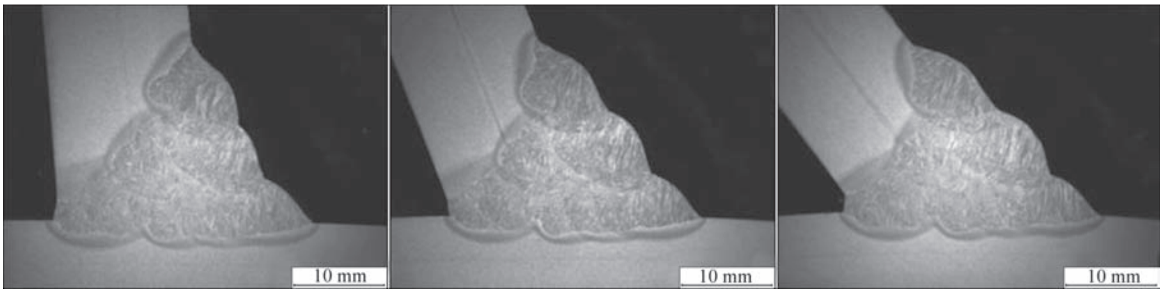

Figure 7. Macrosections on a robotic T-joint weld

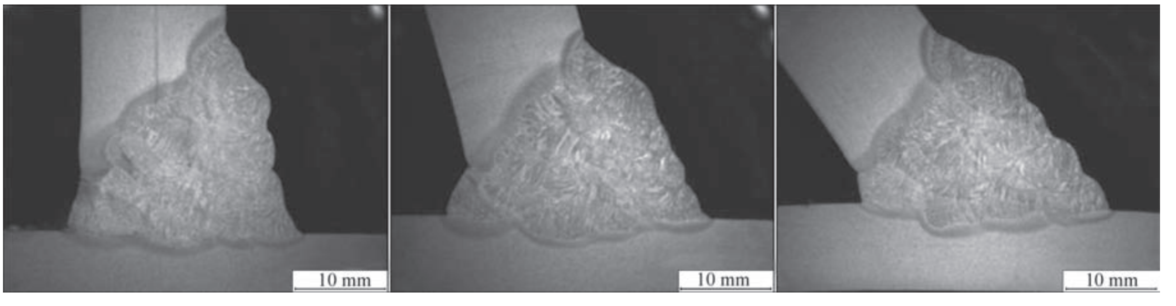

Figure 8. Macro sections on a manual T-joint weld

on the example tube node above in order to assess weld and root fusion quality, see Figure 7 and Figure 8.

The macrosections show that the root weld was not easy for the welder either; this type of work requires extensive training and experience as well as excellent judgement. The test also showed that automation may lead to a favourable outcome on constant gap dimensions. Constant welding speed combined with continuous component movement also increased the deposition rate, thus halving the number of weld layers.

Summary and outlook. The tests carried out in the project have shown that fully mechanised multi-layered MIG/MAG welding is possible on tube joints. The weld quality achieved represents a leap in both geometric and visual quality as well as in material properties, so the findings will be used in further studies planned for this topic. The research findings define the influencing factors determined and possible approaches in performing these complex welding jobs using robots. We intend to research approaches into more detailed issues such as root welding with varying gaps or welding on oblique tube nodes together with the project partners we have been working with so far and new project partners. Implementation on root welds with varying gaps or other joint types (oblique joints) promises a high level of potential in financial terms as shown in initial theoretical economic comparisons using the welded tube nodes as an example. Comparison between manual and robotic welding showed production time savings of around two-thirds. These studies and findings are also of great economic importance in demonstrating automation options as an alternative in view of the apparent lack of qualified welders on the market.

Acknowledgements. *We would like to express our gratitude to the German Federal Ministry of Economics and Technology (BMWi) and EuroNorm as the project owner for their support in our research. We would especially like to thank the companies that participated in these studies:*

- ZIS Industrietechnik GmbH;
- Ibs Automation GmbH;
- Falldorf Sensor GmbH;
- EWM AG.

1. http://www.zis-meerane.de/software/tubecut/

Received 13.11.2018